Journal of Alloys and Compounds 480 (2009) 928–933

Contents lists available at ScienceDirect

Journal of Alloys and Compounds

journal homepage: www.elsevier.com/locate/jallcom

Combustion synthesis of hexagonal AlN–SiC solid solution under low nitrogen pressure

R.-C. Juang [1], C.-C. Chen *, J.-C. Kuo, T.-Y. Huang, Y.-Y. Li [2]

Chaoramics Laboratory, Department of Chemical Engineering, National Chung Cheng University, Chia-Yi 621, Taiwan

ARTICLE INFO

Article history:
Received 17 September 2008
Received in revised form 15 February 2009
Accepted 21 February 2009
Available online 4 March 2009

Keywords:
Ceramics
Nitride materials
Solid state reactions
Microstructure

ABSTRACT

AlN–SiC solid solutions were synthesized by self-propagating combustion of powders consisting of Al, Si and carbon black (CB) under low nitrogen pressure (0.1–0.5 MPa), with the molar ratio of Al and Si, and nitrogen pressure as the main investigating parameter. The products were mainly AlN–SiC solid solution with a residual Si, and the morphology was of hexagonal crystal. Nearly pure AlN–SiC solid solution, also having the best solid-solution homogeneity in this study, was obtained by adding extra CB to the starting powders. The best Al/Si molar ratio was 1 or 1.5 and the combustion results indicated that better combustion produced a higher combustion temperature, greater product purity, and better solid solution homogeneity. Increasing nitrogen pressure (from 0.1 to 0.5 MPa) moderately increased the combustion temperature and the product homogeneity, but combustion velocity increased by around 65%. The full width at half maximum (FWHM) of AlN–SiC solid solution's (1 1 0) XRD peak, served as the homogeneity index for the AlN–SiC solid solution (D. Kata, K. Shirai, M. Ohyanagi, Z.A. Munir, J. Am. Ceram. Soc. 84 (2001) 726–732.), of all samples were summarized with the reported values in the literature, where our FWHM values were comparable to the reported data.

1. Introduction

Aluminum nitride (AlN) is a promising advanced ceramic because of its excellent physicochemical properties, such as high thermal conductivity, high electrical resistance, low dielectric constant, low thermal expansion coefficient, good thermal shock resistance, as well as good corrosion resistance [2–5]. Therefore, AlN is especially considered for many heat-dissipation applications such as IC packaging materials, heat sink, and high thermally conductive composites. AlN and Silicon carbide (SiC) have similar 2H wurtzite-type structures, and closely-matched lattice parameters (AlN: $a = 3.111$, $c = 4.979$; 2H–SiC: $a = 3.076$, $c = 5.048$, unit in Å). Therefore, Culter et al. [6] proposed that AlN and SiC could form a complete solid solution (denoted as AlN–SiC) to increase the mechanical properties due to their similar structures and high-temperature properties.

AlN–SiC has been prepared by several methods, including carbothermal reduction of a mixture of silica, alumina and carbon powders under nitrogen, and hot-pressing a mixture consisting of SiC and AlN powders under high nitrogen pressure [7,8]. Recently, combustion synthesis (CS) or self-propagating high-temperature synthesis (SHS) has been utilized to cost-effectively prepare the AlN–SiC solid solution. Xue and Munir [9] fabricated the solid solution via reaction between silicon nitride (Si_3N_4), Al, and C powders under an electric field. Using Si_3N_4 as a reactant, they demonstrated that solid solution could be produced in a self-sustaining combustion regime under an ambient nitrogen pressure (0.1 MPa) without an electric field [1]. Other schemes included combustion of powder mixtures of Al, Si, and carbon in nitrogen [10,11]. It is noted that residue Si was always present in the final product in above studies. More recently, powders of AlN–SiC solid solution was prepared through nitriding combustion of Al, C, and Si_3N_4 powders in air [13]. Dense 2H AlN–SiC solid solution was obtained by the post-heat treatment of dense AlN–SiC composites prepared by spark plasma sintering [14], where AlN–SiC samples with different phases were obtained. Because of the importance of AlN–SiC system, properties (mechanical, thermal, and oxidation behavior) of ternary composites (AlN–SiC–TiB_2 [15], ZrB_2–SiC–AlN [16] and AlN–BN–SiC [17]) prepared by different methods have been examined.

Previously, we have successfully prepared hexagonal AlN crystals containing a small amount of residual carbon by combusting a powder mixture of Al and carbon black (CB) [12] and by combusting the Al_4C_3 powders [18] as well, all under low nitrogen pressure (<0.5 MPa). CB served as a dispersion agent to avoid Al coalescence, and remained in the AlN product. In this study, Si powder was added to the starting powder in order to react with the CB to form SiC. Because CB particles are well dispersed in AlN, the

* Corresponding author. Tel.: +886 5 2720411x33462; fax: +886 5 2721206.
E-mail address: chmccc@ccu.edu.tw (C.-C. Chen).
[1] Present address: Department of Energy and Environment Research Laboratories, Industrial Technology Research Institute, Hsinchu, Taiwan.
[2] Nanofabrication laboratory.

0925-8388/$ – see front matter © 2009 Elsevier B.V. All rights reserved.
doi:10.1016/j.jallcom.2009.02.102

formed SiC and the surrounding AlN will have a great opportunity to form a uniform AlN–SiC solid solution with a hexagonal morphology. Effects of the molar ratio (Al/Si) and nitrogen pressure on the microstructure, combustion temperature and velocity, as well as product homogeneity were examined.

2. Experimental procedures

Al powder (<30 μm, 99.7% pure, Strem Chem.) and Si powder (<40 μm, 99.5%, Alfa Aesar), CB powder (aggregated size < 10 μm, 99.9% pure, China Synthetic Rubber) were used as the reactant. The commercial β-SiC powder (<40 μm, 99% pure, Strem Chem.) and AlN powder (<10 μm, 98%, Acros Organics) were used for comparison. Nitrogen was 99.99% pure. The formation of AlN–SiC solid solution follows the reaction:

$$Al + Si + CB + 1/2N_2 \rightarrow AlN\text{–}SiC.$$

The reactant mixture consisted of Al, Si and CB powders, where the molar ratio between Si and CB was 1:1 and the Al amount varied. The molar ratio of Al and Si, denoted as Al/Si, ranging from 0.5 to 2.5 was one of the parameters in this study. Reactant powders were thoroughly mixed in a grinder for 30 min. The powder mixture was placed in a cylindrical Al cup, 12 and 14 mm in diameter and height respectively, made from Al foil. To facilitate nitrogen infiltration, the Al cup was made porous by punching several hundred tiny holes around the surfaces. The Al cup, contained the reactant mixture, was placed into a reaction chamber filled with nitrogen at a controlled pressure ranged from 0.1 to 0.5 MPa.

A tungsten coil, placed 2 mm above the reactant powders, was used as the heat source (the heating power was kept at 1500 W) to trigger the reaction. The electrical power was shut off immediately when the ignition started.

A pyrometer (Chino, IR-AHS, temperature range 800–3300 K) equipped with a data acquisition system recorded the combustion temperature. The combustion sequences, recorded by a high-speed charge couple device (CCD, Toshiba, jk-c40), were monitored and stored in a VCR. Locations of the combustion waves and the associated elapsed time from the recorded combustion snapshots were used to determine the combustion velocity.

The product morphology and phase constitution were analyzed using a scanning electron microscopy (SEM, Jeol, JSM-5410) and X-ray diffractometer (XRD, Shimadzu, XRD-6000), respectively.

3. Results and discussion

The combustion temperature (T_c) and combustion velocity (v) are shown in Fig. 1, where both T_c and v have similar trends (because they are kinetically related) and reached their respective maximum at Al/Si = 1.5. A phase diagram for AlN and SiC system has been experimentally obtained [19], stating that a critical temperature around 2123 K separated the stable solid solution region (denoted as 2H) and the metastable region, which tended to separate into AlN-rich and SiC-rich phase (denoted as δ_1 and δ_2, respectively). For temperature above 2123 K, the AlN and SiC system located in the 2H stable solid solution region. Table 1 summarizes combustion temperature data and the corresponding phases for different Al/Si. When Al/Si was respectively 1, 1.5 and 2, the combustion temperature exceeded the critical temperature of 2123 K, indicating the as-prepared products were all stable AlN–SiC solid solution. On the other hand, when Al/Si was 0.5, 0.75 or 2.5, the low combustion temperature resulted in a metastable solid solution.

Table 1
Summary of combustion temperature and associated phases for different Al/Si molar ratio.

Al/Si (mol. ratio)	Phase diagram (mol.% AlN)	T_c (K)	Phase region
0.5	33.33	1972	$\delta_1 + \delta_2$
0.75	42.85	2011	$\delta_1 + \delta_2$
1	50	2150	2H–SS
1.5	60	2287	2H–SS
2	66	2142	2H–SS
2.5	71.42	2115	$\delta_1 + \delta_2$

Fig. 2 shows the XRD patterns of a green mixture (Al:Si:CB = 1:1:1) and as-prepared products for different Al/Si molar ratio under 0.3 MPa nitrogen pressure. The XRD patterns

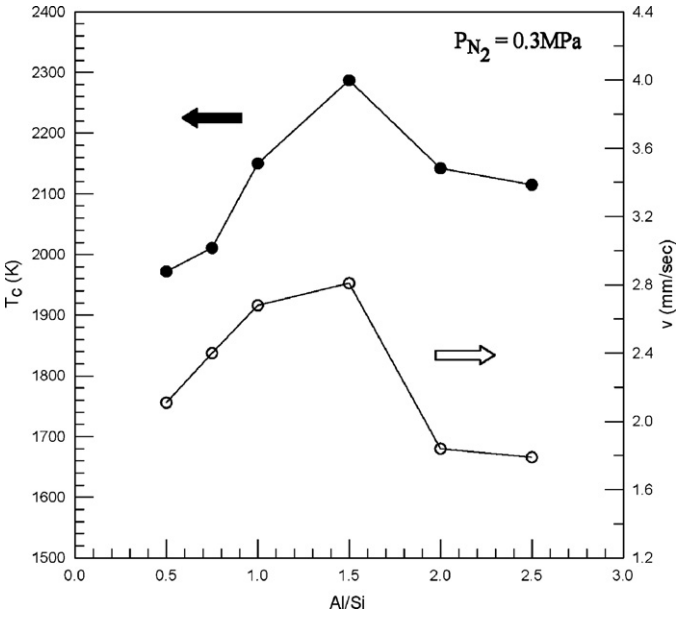

Fig. 1. Combustion temperature and velocity varied with Al/Si molar ratio under 0.3 MPa nitrogen pressure.

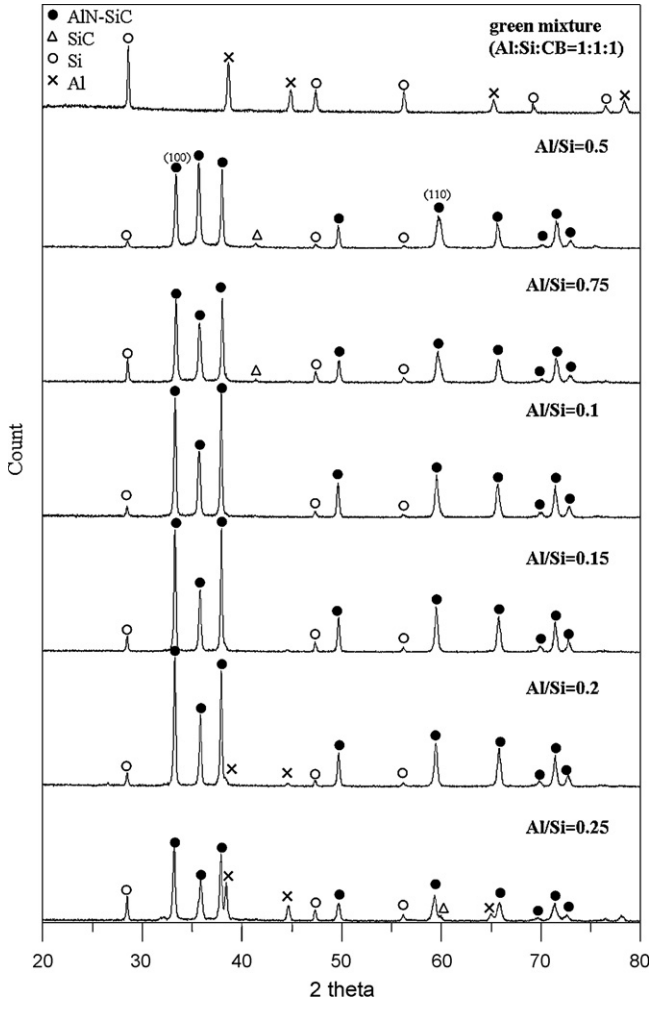

Fig. 2. XRD patterns of a green mixture and the as-prepared products varied with Al/Si molar ratio under 0.3 MPa nitrogen pressure.

revealed the main constituent was AlN–SiC solid solution. Compared to combusted samples, the XRD pattern of green mixture has a broad band (above the baseline) ranging from 20 to 35°, contributed from the small-sized CB. For Al/Si less than 1, the as-prepared products consisted of the main AlN–SiC solid solution, residual Si and trace of SiC, indicating excess Si and carbon. For Al/Si at 1 and 1.5, intensity of AlN–SiC peaks greatly increased probably due to the higher combustion temperature. SiC was almost invisible, but an extremely small amount of Al emerged when Al/Si was 1.5. The intensity of Si decreased and residual Si still existed in the product probably resulted from aluminum loss at the elevated temperature, due to aluminum's low melting point. This imperfection was remedied and will be addressed shortly. When Al/Si further increased to 2 and 2.5, the AlN–SiC solid solution deteriorated from the decreased AlN–SiC peaks and emerging Al peaks. Solid solution deterioration became more severe when the molar ratio was 2.5, having the largest amount of excess Al. Because the Si and CB ratio maintained at 1:1, therefore the relative amount of CB dispersion agent was smaller when Al/Si increased. Due to less dispersion available, Al coalescence was severe resulting in poor combustion performance. This is also the reason for decreased combustion temperature decreased when excess Al was in the green mixture. Single-phase SiC was detected for the green mixtures containing excess Si (Al/Si = 0.5 and 0.75) and having Al coalescence (Al/Si = 2.5). For good combustion cases to yield a good AlN–SiC solid solution, Si and C atoms were incorporated into the AlN–SiC solid solution such that no single-phase SiC was detected. Concluding from the above results, the best Al/Si molar ratio was 1 or 1.5. Compared to the best Al/Si cases, the main peak of AlN–SiC shifted a little for the other molar ratios.

In addition to the phase constituent in the products, the most important property for the solid solution is its homogeneity. The FWHM of the (1 1 0) peak of AlN–SiC has been proposed [1] as a good homogeneity index for the AlN–SiC solid solution. When the FWHM value is smaller, solid solution homogeneity is better. The previously mentioned lattice structure similarity between the hexagonal AlN and 2H-SiC results in only small differences in their XRD patterns (hexagonal AlN, JPCD card no. 25-1133; 2H SiC, JPCD card no. 29-1130), except for a unique diffraction peak of 2H–SiC at $2\theta = 41.383°$. Compared to other diffraction peaks, the difference between the AlN's and 2H–SiC's (1 1 0) is the largest among the dominant diffraction peaks so that it is relatively convenient to use (1 1 0)'s FWHM as the index to describe the AlN–SiC solid solution homogeneity. The fine scans were carried out from 58 to 61° around the (1 1 0) peak. Fig. 3a shows the enlarged (1 1 0) peak for Al/Si as 1, where an obvious right shoulder presented near the (1 1 0) peak. This shoulder results from the Cu $K\alpha_2$ irradiation producing the unsymmetrical (1 1 0) peak via diffraction peak superposition from $K\alpha_1$ and $K\alpha_2$ irradiations. Normally, the $K\alpha_2$ irradiation is unimportant and negligible because it is extremely close to the $K\alpha_1$ irradiation since the wavelength difference between Cu $K\alpha_1$ and $K\alpha_2$ is only around 0.004 Å. However, Kα2 irradiation readily affects the (1 1 0)'s FWHM accuracy because of the extremely small range of the diffraction angle shown in Fig. 3a. Hence, the diffraction from $K\alpha_2$ irradiation for all samples is removed using the X-ray diffractometer software. After removing the diffraction peaks by $K\alpha_2$ irradiation, the (1 1 0) peaks for various Al/Si shown in Fig. 3(b)–(g) were symmetrical. In Fig. 3, the peak gradually shifted to the left as Al/Si increased. For comparison purpose, the (1 1 0) peak of the sample under the best molar ratio (Al/Si = 1 or 1.5) was used as the reference. The (1 1 0) peak shifted to the right for smaller molar ratios, while it shifted to the left for the larger molar ratios. Right- and left-shifted peaks respectively indicated the sample was SiC-rich and AlN-rich solid solution.

The FWHM also depends on the crystallinity and size of particles. Particle size and crystallinity is typically determined from the structure of the most dominant peak. From the sharp (1 0 0) peaks shown in Fig. 2, the crystallinity of the as-prepared samples was all pretty good. Fig. 4 also shows that the (1 0 0)'s FWHM was relatively uniform, suggesting that AlN–SiC grain size did not differ greatly. Fig. 4 also shows the variation of (1 1 0)'s FWHM was greater than that of (1 0 0)'s. This is unusual that the FWHM variation of a less dominant peak is greater than that of the most dominant peak. Using the (1 1 0)'s FWHM to describe the homogeneity of the AlN–SiC solid solution is acceptable under the similar crystallinity and grain size. The measured FWHM values for different Al/Si were given in Fig. 4, showing the lowest FWHM occurred at Al/Si = 1.5. Recalling the results of combustion temperature (Fig. 1), XRD patterns (Fig. 2) and FWHM (Fig. 4), it is consistent that a better combustion results in a higher combustion temperature, larger product purity, and a better homogeneity of solid solution as well. The FWHM curve in Fig. 4 is almost inverse to the combustion temperature curve in Fig. 1. A better combustion not only produces a better product purity and homogeneity but also has a better morphology. Fig. 5 shows the SEM images of as-prepared products for different Al/Si. Agglomerates of fine particles were observed for small values of Al/Si (0.5 and 0.75). When Al/Si reached 1, a hexagonal-like crystal began to emerge. A better crystal structure was obtained for larger Al/Si (1.5 and 2), compared to the cases for Al/Si at 0.5 and 0.75. As for the sample with excess Al (Al/Si = 2.5), the morphology became aggregated crystalline structure owing to excess Al.

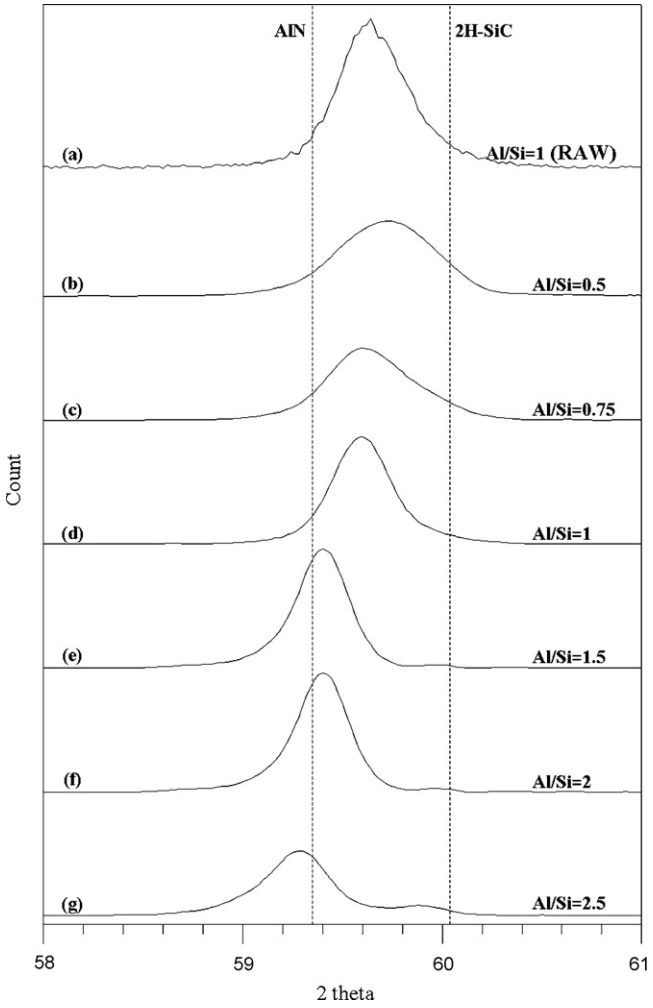

Fig. 3. Enlargement of (1 1 0) peak of AlN–SiC solid solution for different Al/Si. (a) Original data, (b)–(g) data after removing the diffraction peak from the $K\alpha_2$ irradiation.

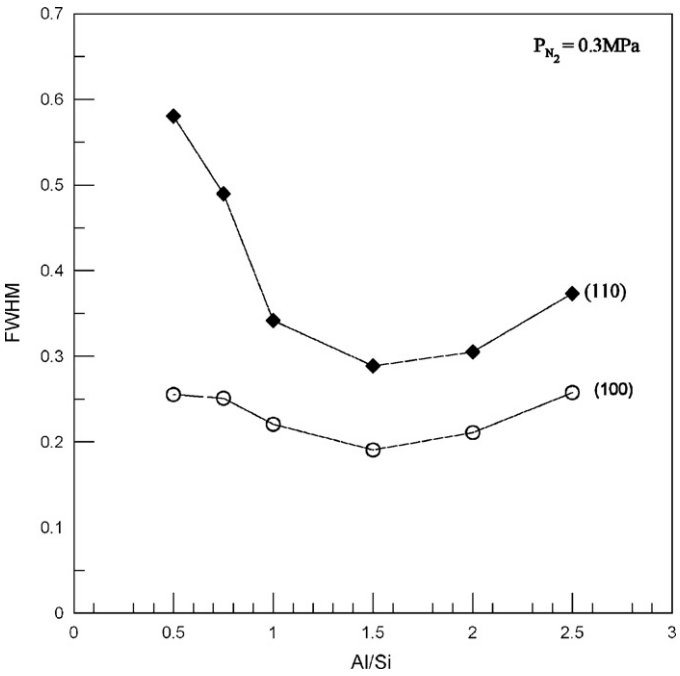

Fig. 4. Effect of Al/Si molar ratio on the FWHM of (1 1 0) and (1 0 0) planes of AlN–SiC solid solution. Nitrogen pressure is 0.3 MPa.

As mentioned previously, a residual Si remained in the AlN–SiC product. An experiment was carried out with Al/Si as 1, where extra CB was added to react with the residual Si. Fig. 6 shows the XRD pattern and microstructure of the as-prepared AlN–SiC solid solution (molar ratio Al: Si:CB = 1: 1: 1.2) under 0.3 MPa nitrogen pressure. The XRD pattern in Fig. 6a shows product purity as extremely high,

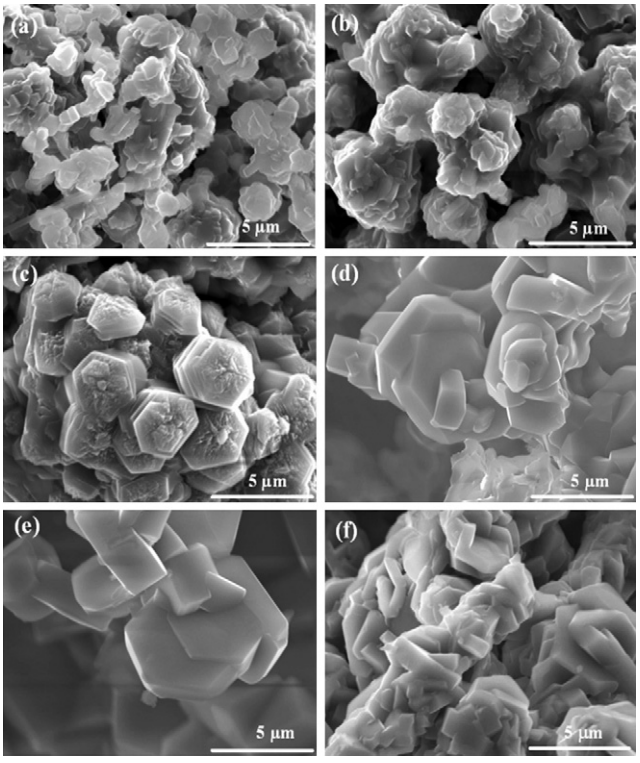

Fig. 5. SEM micrographs of as-prepared products. Al/Si = (a) 0.5, (b) 0.75, (c) 1, (d) 1.5, (e) 2, (f) 2.5.

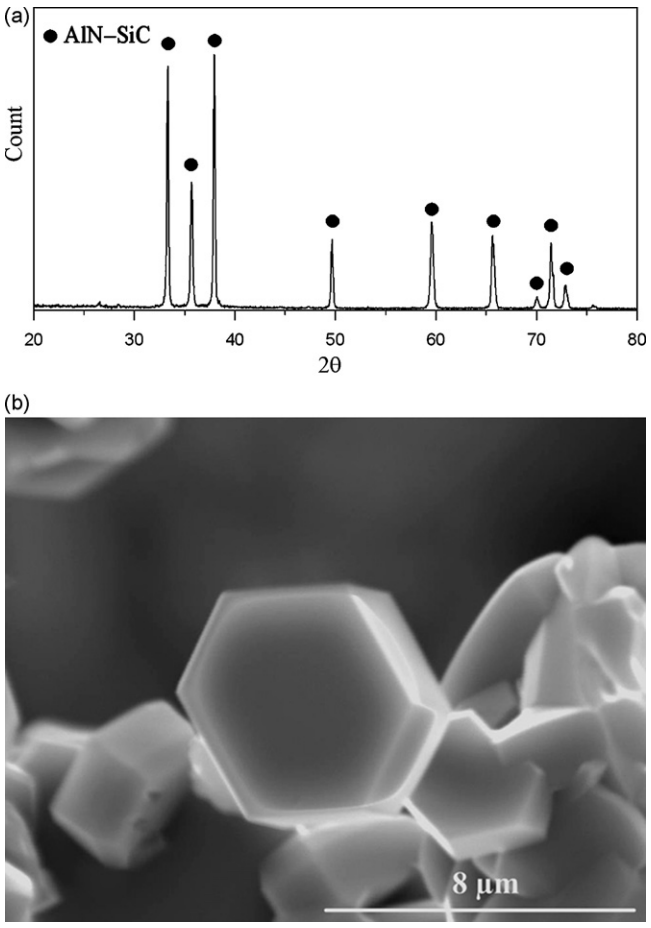

Fig. 6. Sample prepared by combusting powders with the molar ratio Al:Si:CB = 1:1:1.2 under 0.3 MPa nitrogen pressure: (a) XRD pattern, (b) SEM micrograph.

almost pure AlN–SiC solid solution. This result indicated that residual Si can be removed very efficiently simply by adding extra CB. Moreover, FWHM of this high-purity sample was 0.271, which was the lowest value in this study. The SEM image in Fig. 6b shows

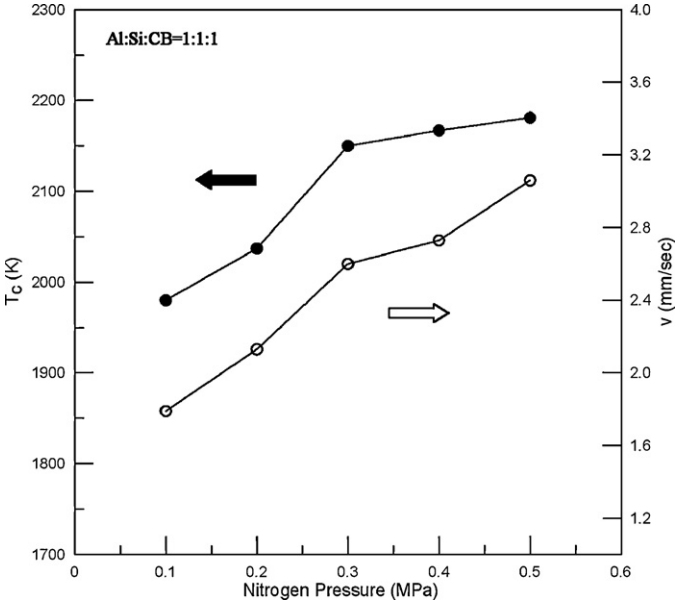

Fig. 7. Effects of nitrogen pressure on the combustion temperature and velocity.

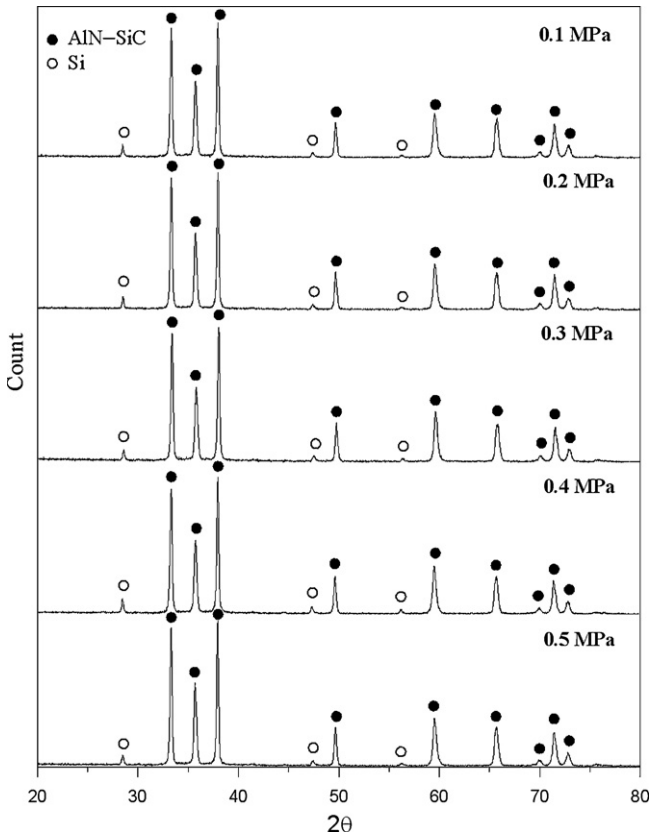

Fig. 8. XRD patterns of as-prepared products under different nitrogen pressure. Al/Si = 1.

a single hexagonal AlN–SiC crystal, suggesting a lower degree of aggregation.

The effects of nitrogen pressure on the combustion were also investigated. Fig. 7 shows moderately increasing combustion temperature and velocity with increasing nitrogen pressure. When nitrogen pressure increased from 0.1 to 0.5 MPa, combustion temperature increased about 200 K while combustion velocity increased to around 65%. The increase of nitrogen pressure readily facilitates nitrogen diffusion to enhance combustion. Fig. 8 shows the XRD patterns of products under different nitrogen pressure (Al:Si:C = 1:1:1). These XRD results were not influenced by the nitrogen pressure in the range from 0.1 to 0.5 MPa. However, the solid solution homogeneity slightly increased reflected by the small decrease of FWHM (Fig. 9) as increasing nitrogen pressure increased. All the obtained FWHM values in this study and those available in the literature [8,9,11,20] were summarized in Fig. 10. Although our FHWM values are not better than the reported values, they are comparable. The morphology of as-prepared AlN–SiC solid solution is also hexagonal, which is different from the usual sphere-like shape reported in the literature.

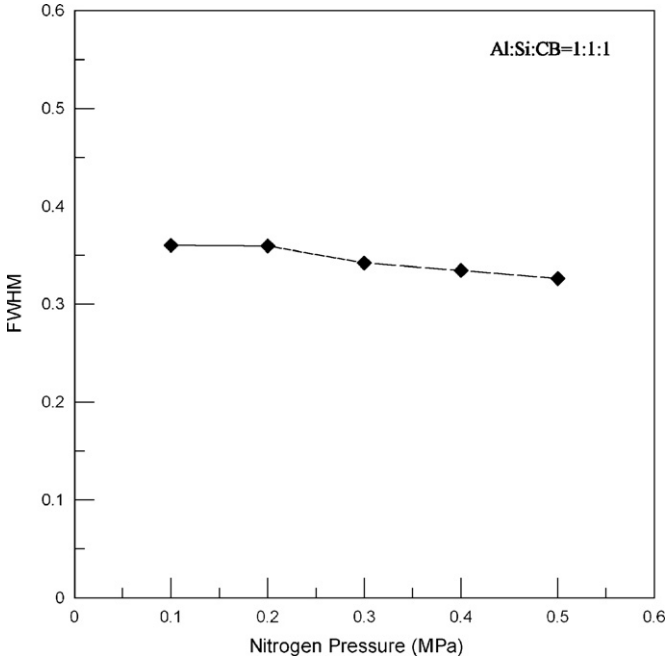

Fig. 9. Effect of nitrogen pressure on the FWHM value of AlN–SiC's (1 1 0) plane.

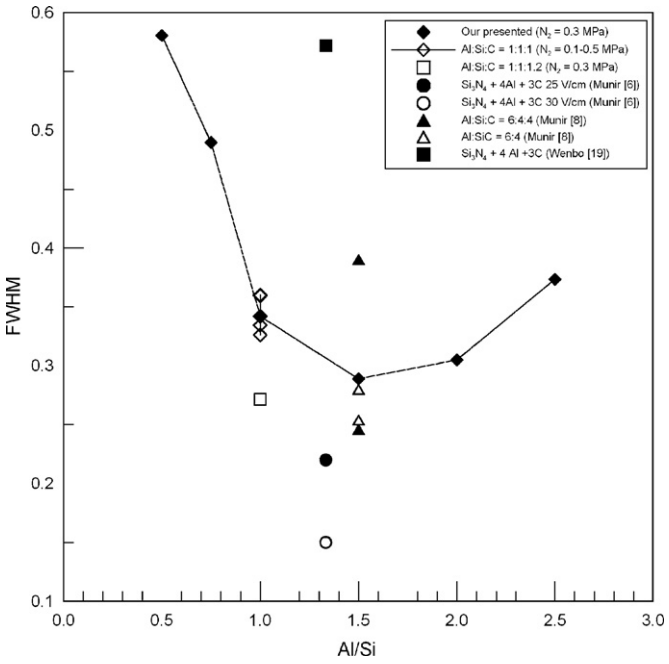

Fig. 10. Summary of FWHM values in this study and available in literature.

4. Conclusions

Hexagonal AlN–SiC solid solutions were successfully obtained by self-propagating combustion of powders consisting of Al, Si and CB under low nitrogen pressure. The products were mainly AlN–SiC solid solution with a residual Si, and the product morphology was of hexagonal shape. A nearly pure AlN–SiC solid solution, also having the best solid-solution homogeneity, was obtained by adding extra CB to the starting powders. The best Al/Si molar ratio was 1 or 1.5, indicating a better combustion results in larger combustion temperature, greater product purity, and better solid solution homogeneity. Increasing nitrogen pressure moderately increased combustion temperature and product homogeneity, but combustion velocity increased by around 65%. The obtained FWHM values of all samples were summarized with the reported values in the literature, where our FWHM values were comparable to reported values.

Acknowledgement

This work was supported by the National Science Council of Republic of China under Grant No. NSC 95-2221-E-194-083-MY2.

References

[1] D. Kata, K. Shirai, M. Ohyanagi, Z.A. Munir, J. Am. Ceram. Soc. 84 (2001) 726–732.
[2] G.A. Slack, R.A. Tanzilli, R.O. Pohl, J.W. Vandersande, J. Phys. Chem. Solids 48 (1987) 641–647.
[3] R. Bachelard, P. Joubert, Mater. Sci. Eng. A 109 (1989) 247–251.
[4] Z.C. Jou, A.V. Virkar, J. Am. Ceram. Soc. 73 (1990) 1928–1935.
[5] L.M. Sheppard, Am. Ceram. Soc. Bull. 69 (1990) 1801–1812.
[6] J.B. Cutler, P.D. Miller, W. Rafaniello, H.K. Park, D.P. Thompson, K.H. Jack, Nature 275 (1978) 434–435.
[7] W. Rafaniello, K. Cho, A.V. Virkar, J. Mater. Sci. 16 (1981) 3479–3488.
[8] R. Ruh, A. Zangvil, J. Am. Ceram. Soc. 65 (1982) 260–265.
[9] H. Xue, Z.A. Munir, J. Eur. Ceram. Soc. 17 (1997) 1787–1792.
[10] C. Kexin, J. Haibo, H.P. Zhou, J.M.F. Ferreira, J. Eur. Ceram. Soc. 20 (2000) 2601–2606.
[11] M. Ohyanagi, K. Shirai, N. Balandina, M. Hisa, Z.A. Munir, J. Am. Ceram. Soc. 83 (2000) 1108–1112.
[12] R.-C. Juang, C.-J. Lee, C.-C. Chen, Mater. Sci. Eng. A 357 (2003) 219–227.
[13] L. Mei, J.-T. Li, Acta Mater 56 (2008) 3543–3549.
[14] R. Kobayashi, J. Tatami, T. Wakihara, K. Komeya, T. Meguro, J. Am. Ceram. Soc. 91 (2008) 1548–1552.
[15] L. Zhou, Y. Zheng, S. Du, H. Li, J. Alloys Compd. (2008) doi:10.1016/j.jallcom.2008.11.090.
[16] Y. Wang, J. Liang, W. Han, X. Zhang, J. Alloys Compd. (2008) doi:10.1016/j.jall.com.2008.08.001.
[17] A.A. Buchheit, G.E. Hilmas, W.G. Fahrenholtz, D.M. Deason, H. Wang, Mater. Sci. Eng. A 494 (2008) 239–246.
[18] R.-C. Juang, C.-C. Chen, Mater. Sci. Eng. A 458 (2007) 210–215.
[19] A. Zangvil, R. Ruh, J. Am. Ceram. Soc. 71 (1988) 884–890.
[20] W.B. Bu, J. Xu, T. Qiu, X.Y. Li, J. Mater. Sci. Lett. 21 (2002) 731–732.